Journal of Physiology - Paris xxx (2012) xxx–xxx

Contents lists available at SciVerse ScienceDirect

Journal of Physiology - Paris

journal homepage: www.elsevier.com/locate/jphysparis

Review Article

Propagating waves in thalamus, cortex and the thalamocortical system: Experiments and models

Lyle Muller *, Alain Destexhe

Unité de Neurosciences, Information, et Complexité (UNIC), CNRS, Gif-sur-Yvette, France

ARTICLE INFO

Article history:
Available online xxxx

Keywords:
Voltage-sensitive dye
Multi-electrode array
Population dynamics
Propagating waves
Oscillations
Sensory cortices
Spiking neural networks

ABSTRACT

Propagating waves of activity have been recorded in many species, in various brain states, brain areas, and under various stimulation conditions. Here, we review the experimental literature on propagating activity in thalamus and neocortex across various levels of anesthesia and stimulation conditions. We also review computational models of propagating waves in networks of thalamic cells, cortical cells and of the thalamocortical system. Some discrepancies between experiments can be explained by the "network state", which differs vastly between anesthetized and awake conditions. We introduce a network model displaying different states and investigate their effect on the spatial structure of self-sustained and externally driven activity. This approach is a step towards understanding how the intrinsically-generated ongoing activity of the network affects its ability to process and propagate extrinsic input.

Contents

1. Introduction

Recent years have seen an increase in measurements of large-scale spatiotemporal dynamics of neocortical networks, due to improvements in voltage-sensitive dye (VSD) (Shoham et al., 1999) and in multielectrode array (MEA) (Maynard et al., 1997) technologies. With these technological advancements, it is now generally possible to use single-trial imaging to observe the detailed dynamics of cortical circuits, whose trial-to-trial variability may preclude measurement by averaging techniques. Following preliminary evidence from electrophysiological and optical imaging studies *in vitro* (Chagnac-Amitai and Connors, 1989; Langdon and Sur, 1990; Hirsch and Gilbert, 1991; Metherate and Cruikshank, 1999; Sanchez-Vives and McCormick, 2000; Wu et al.,

* Corresponding author.
E-mail address: muller@inaf.cnrs-gif.fr (L. Muller).

0928-4257/$ - see front matter © 2012 Elsevier Ltd. All rights reserved.
http://dx.doi.org/10.1016/j.jphysparis.2012.06.005

2001; Huang et al., 2004; Pinto et al., 2005), VSD and MEA experiments have provided direct observations of spatiotemporally coherent population activity in many cortical areas, anesthetic states, and stimulation conditions. For example, propagating waves have been observed *in vivo* in the visual (Grinvald et al., 1994; Kitano et al., 1994; Slovin et al., 2002; Jancke et al., 2004; Xu et al., 2007; Ahmed et al., 2008; Han et al., 2008; Nauhaus et al., 2009), somatosensory (Derdikman et al., 2003; Petersen et al., 2003; Civillico and Contreras, 2006), auditory (Reimer et al., 2010); and motor (Rubino et al., 2006) cortices under both spontaneous and evoked conditions. These diverse observations suggest that propagating waves could potentially be a general phenomenon in the large-scale dynamics of neocortex. These results, however, have been obtained under a myriad of anesthetic conditions and brain states, and a unified account of the dependence of propagating waves on network state has not yet emerged. It is therefore necessary to first determine the relationship of propagating waves to awake, activated brain states.

In the present paper, we first review the experimental literature from multichannel recording techniques, focusing specifically on propagating activity in thalamic, cortical and thalamocortical networks. In cortical networks, we also emphasize the brain state involved in each study, to assess the functional relevance of propagating waves to the awake brain. The critical factor in determining a network's responsiveness to perturbations is its conductance state (Destexhe and Paré, 1999; Destexhe et al., 2003), as the conductance state determines the average membrane potential throughout the network and the driving force on a single input, given a fixed conductance change at the synapse. Changes in global brain state, such as anesthesia or arousal (from sleep to wake), affect the spatiotemporal dynamics of cortical networks via changes in conductance state. Thus, we will analyze changes in brain state within the framework of conductance-based effects at the network level. We will focus mainly on experimental results from primary visual cortex and refer to the results from other brain areas (auditory, somatosensory, motor) for purposes of comparison. We also review both experiments and models of propagating waves in thalamic, cortical and thalamocortical networks. Finally, we present preliminary results from a computational study using network models of nonlinear adaptive exponential integrate and fire (AdEx) neurons (Brette and Gerstner, 2005). Neuronal adaptation has previously been shown to be critical for modeling the transition between UP/DOWN and AI states (Destexhe, 2009); here, we study the contributions of neuronal adaptation to low-frequency activity (1–4 Hz) and excitatory/inhibitory (E/I) interactions to high-frequency activity (20–80 Hz) as parallel factors determining the network state. Moreover, because the adaptation variable in the AdEx model has a straightforward interpretation in terms of specific membrane conductances (K^+), which are also those affected by many anesthetic drugs (Sanchez-Vives and McCormick, 2000; Franks, 2008; Destexhe, 2009), a connection among basic pharmacology, brain state, and spatiotemporal network dynamics becomes possible.

2. Propagating waves in different networks and network states

2.1. In vitro

The possibility of coherent propagating activity was first raised by VSD, MEA, and intracellular studies *in vitro*. Though some studies have used disinhibited slices to study the spatial component of epileptiform activity (Chagnac-Amitai and Connors, 1989; Huang et al., 2004; Pinto et al., 2005), many studies have observed propagating activity in pharmacologically normal slices (Langdon and Sur, 1990; Hirsch and Gilbert, 1991; Metherate and Cruikshank, 1999, Wu et al., 2001). It is well known that neurons *in vitro*, which lack a large fraction of synaptic input, have low membrane potentials and high input resistances (Cruikshank et al., 2007) compared to those measured *in vivo* (Steriade et al., 2001), similar to a neocortical DOWN state (Steriade et al., 1993; Destexhe et al., 2003). Propagating activity *in vitro* is typically initiated by means of electrical stimulation, either directly to cortical areas (Wu et al., 1999, 2001; Buonomano, 2003; Pinto et al., 2005) or to thalamocortical afferents (Metherate and Cruikshank, 1999), although in at least one study activity was stimulated using local application of glutamate (Sanchez-Vives and McCormick, 2000). While these stimuli certainly have different statistics from those induced by the sensory stimulation delivered *in vivo*, these artifically induced depolarizations may serve as a basic pulse perturbation. Because of the quiescent state of these neuronal networks, the driving force on the EPSPs evoked by these stimuli will be strong and synchronously drive many neurons close to spiking threshold. Interestingly, recent evidence *in vitro* also suggests a critical role for the infragranular layers (and interlayer interactions) in supporting the horizontal spread of activity across the cortex (Wester and Contreras, 2012).

The pharmacological dependence of propagating activity has been well-characterized by *in vitro* studies and has been localized to individual receptor classes. Several studies have shown that the non-NMDA glutamatergic ionotropic receptor antagonists CNQX[1] and DNQX[2] block horizontal propagation (Fukuda et al., 1998; Metherate and Cruikshank, 1999; Sanchez-Vives and McCormick, 2000; Wu et al., 2001; Pinto et al., 2005), specifically implicating polysynaptic fast glutamatergic transmission in sustaining propagating activity. NMDA-mediated conductances have also been shown to play a role in horizontal propagation, albeit to a lesser extent, with some studies showing a clear dependence of the generation of propagating activity on these receptors (Metherate and Cruikshank, 1999; Wu et al., 2001) and others showing only a modulatory effect (Fig. 1A) (Fukuda et al., 1998; Sanchez-Vives and McCormick, 2000). Blockage of $GABA_A$ receptors has a dramatic affect on neuronal activity, transforming normal horizontal propagation into epileptiform activity (Wu et al., 2001; Pinto et al., 2005), speeding up the propagation (from 11 ± 6 mm/s to 125 ± 24 mm/s – Fig. 1B), and focusing activity around the wavefront.

Combined with intracellular studies of horizontal axonal conduction, which falls in the range of 100–500 mm/s for unmyelinated intracortical fibers across species and cortical areas (Bringuier et al., 1999; Hirsch and Gilbert, 1991; González-Burgos et al., 2000; Murakoshi et al., 1993; Telfeian and Connors, 2003), VSD and MEA studies *in vitro* captured the first estimates of the speed of horizontal propagation of population events across the surface of the cortex (Fukuda et al., 1998). This estimation of propagation speed is in general agreement for the speeds observed *in vivo* (Grinvald et al., 1994; Jancke et al., 2004; Nauhaus et al., 2009), though some studies have reported values one order of magnitude lower in the anesthetized rat (Xu et al., 2007; Han et al., 2008) and slice preparations (Sanchez-Vives and McCormick, 2000; Wester and Contreras, 2012). While the cause for this discrepancy is unclear, possible sources include the vast differences in brain state for individual experiments, species-specific differences between rodents and other mammals, or differing techniques for measuring propagation speed (e.g. center of mass methods (Xu et al., 2007; Han et al., 2008), latency analysis (Tanifuji et al., 1994), and the offset of maximum correlation (Sanchez-Vives and McCormick, 2000)).

[1] 6-Cyano-7-nitroquinoxaline.
[2] 6,7-Dinitroquinoxaline-2,3-diome.

Please cite this article in press as: Muller, L., Destexhe, A. Propagating waves in thalamus, cortex and the thalamocortical system: Experiments and models. J. Physiol. (2012), http://dx.doi.org/10.1016/j.jphysparis.2012.06.005

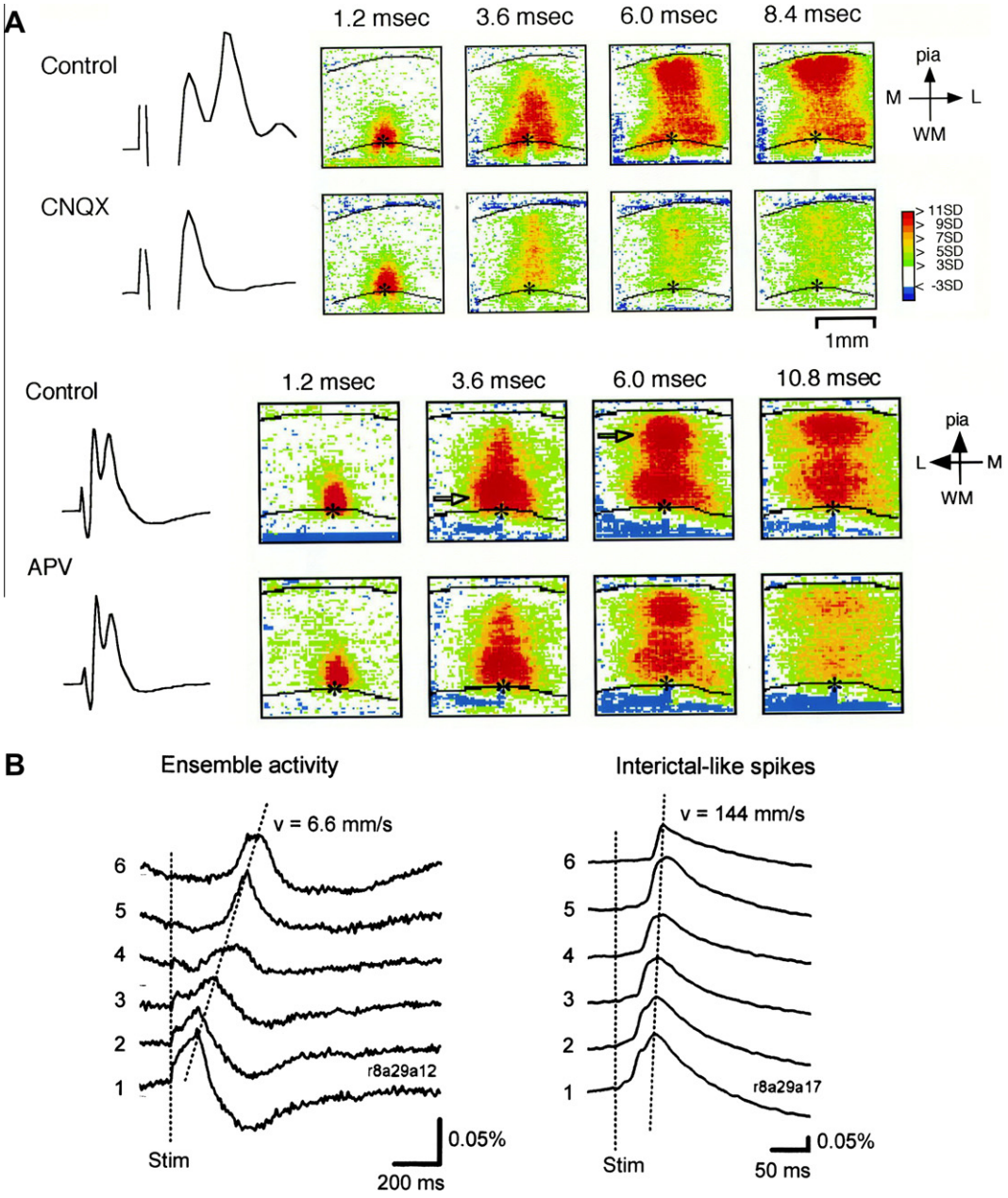

Fig. 1. Propagating activity in cortical slices. (A) Two different pharmacological conditions illustrating clear dependence of horizontal spread of activity on fast glutamatergic synaptic transmission mediated by AMPA receptors (CNQX, bath application) and partial dependence on NMDA-mediated conductances (APV, bath application). Data taken from coronal slices of rat primary visual cortex. Adapted from Fukuda et al. (1998). (B) Measurement of propagation speed with the center of mass method, across normal (ensemble activity) and pharmacologically disinhibited (interictal-like spikes) network states *in vitro*. Adapted from Wu et al. (2001).

Besides cerebral cortex, propagating waves have also been observed *in vitro* in the thalamus, in particular in slices of the visual thalamus of ferrets (Kim et al., 1995) (Fig. 2). Slices comprising the lateral geniculate nucleus (LGN) and the associated reticular sector (perigeniculate nucleus, PGN), as well as their synaptic connections, were shown to display spontaneous spindle waves (von Krosigk et al., 1993). Using multisite extracellular recordings, it was shown that all spindle waves initiate at one side of the slice (sometimes in two sites simultaneously), and propagate in the ventro-dorsal axis. Two types of waves were found, either spindle waves in control conditions, or slow oscillatory waves after blocking $GABA_A$ receptors. These two types of oscillations are compared in Fig. 2B, and both propagate, with the slow oscillation traveling at a lower speed (Kim et al., 1995).

Note that thalamic waves are different from the "monosynaptic" propagating waves of cerebral cortex, which mostly involve a single type of synapse, the excitatory interactions between pyramidal cells. In contrast, thalamic waves rely on the mutual interaction between thalamic relay and reticular nuclei (LGN and PGN here). As we will see in the modeling section, this oscillatory wave activity results from the mutual recruitment of LGN and PGN neurons, which are excitatory and inhibitory, respectively. Thus, thalamic waves involve two types of synapses, and in this sense, they are "polysynaptic" waves. Another consequence is that thalamic waves are difficult to observe because they require slices containing both nuclei and their interconnections, which explains why only one study so far succeeded to obtain this propagating activity *in vitro* (Kim et al., 1995).

Please cite this article in press as: Muller, L., Destexhe, A. Propagating waves in thalamus, cortex and the thalamocortical system: Experiments and models. J. Physiol. (2012), http://dx.doi.org/10.1016/j.jphysparis.2012.06.005

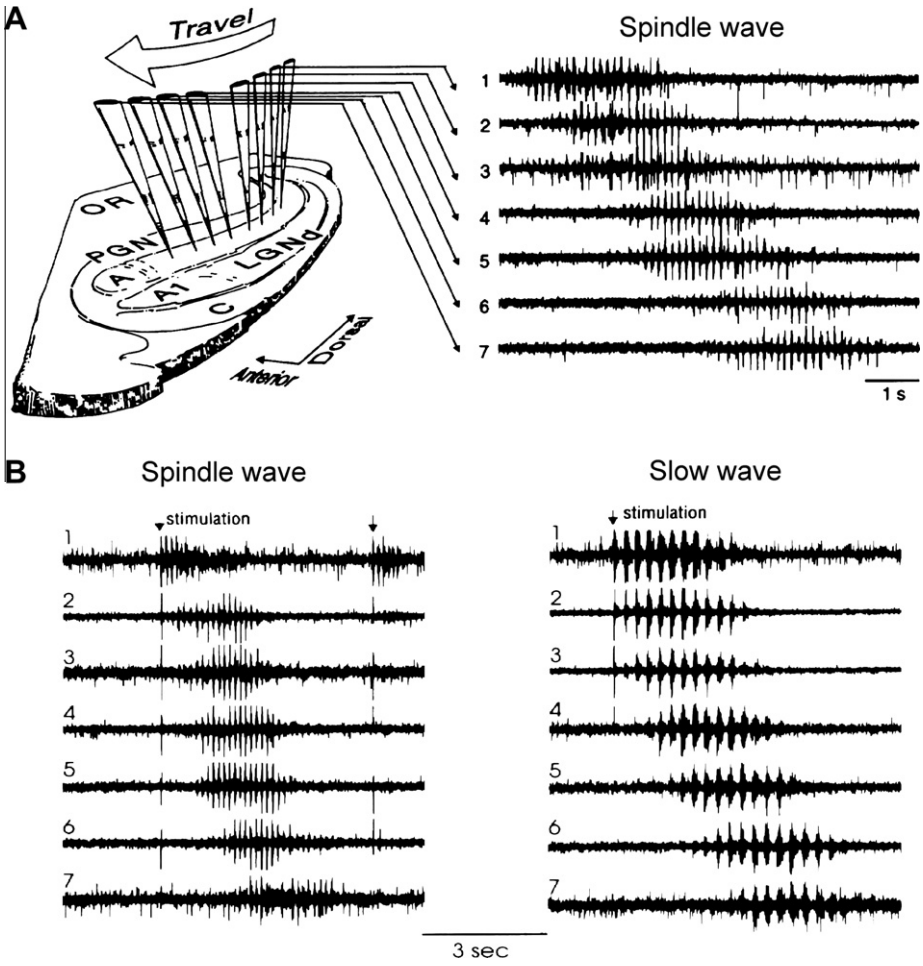

Fig. 2. Propagating waves in thalamic slices. (A) Propagating spindle waves in multisite extracellular recordings in ferret thalamic slices. Spontaneous spindle waves propagate in the ventral–dorsal axis of the slice. (B) Comparison of a spindle wave evoked by electric stimulation (left) with a slow synchronized oscillation obtained after blocking $GABA_A$ receptors (right). In the latter case, the propagation velocity was lower. Modified from Kim et al. (1995).

2.2. In vivo – anesthetized recordings

With multichannel recordings under anesthesia, large, low-frequency spreading depolarization has been observed in the visual cortex of the rat (Xu et al., 2007; Han et al., 2008),[3,4] cat (Jancke et al., 2004; Nauhaus et al., 2009)[5,6] and macaque (Grinvald et al., 1994; Nauhaus et al., 2009),[7,8] lasting hundreds of milliseconds and spreading over the entire cortical area. It is important to distinguish here between propagating waves, which are defined as oscillations propagating across the network, and spreading depolarizations, with a center of mass that remains stationary throughout the response and with a level of activation that decays monotonically with distance. While some studies under anesthetized conditions have observed large, low-frequency propagating waves of activity that spread across the cortical area (Grinvald et al., 1994; Ferezou et al., 2006; Xu et al., 2007; Han et al., 2008), other studies have observed spreading depolarizations (Derdikman et al., 2003; Jancke et al., 2004); the observation of propagating waves in the VSD signal may be dependent on the specific anesthetic level achieved in each study, with more deeply anesthetized preparations favoring large propagating waves, in the case of visual cortex. Additionally, Reimer et al. (2010)[9] have observed propagating waves in the rat auditory cortex on the timescale of 50 ms and traveling across multiple auditory fields under three different anesthetic conditions, and Kral et al. (2009) have observed propagating waves on a similar timescale in the auditory cortex of the cat.

Under anesthesia, these waves generally appear as large single-cycle events in the VSD signal (Fig. 3A) (Ferezou et al., 2006; Xu et al., 2007; Han et al., 2008; Reimer et al., 2010), display repeatable patterns across trials (Jancke et al., 2004; Han et al., 2008; Reimer et al., 2010), and have a dependence on stimulus history (Fig. 3B), both on short (Jancke et al., 2004) and long (Han et al., 2008) timescales. It is interesting to note the dependence on stimulus history in light of the NMDA-mediated conductances that have a modulatory effect on horizontal propagation mentioned above (Fukuda et al., 1998; Metherate and Cruikshank, 1999; Sanchez-Vives and McCormick, 2000; Wu et al., 2001), as a possible indication that organization of synaptic weights on the microscopic level of neuronal activity could have a clear effect on the spatiotemporal dynamics of population events on the macroscopic level of whole cortical areas. The wave generation is generally localized to the point of thalamocortical input (Fig. 3A, left panels), leading to retinotopically (Grinvald et al., 1994; Xu et al., 2007;

[3] Isoflurane.
[4] Pentobarbitol.
[5] Halothane.
[6] Ketamine-xylazine, sodium penthotal, fentanyl, N_2O.
[7] Sodium pentothal.
[8] Sufentanil, propofol.
[9] Either isoflurane, isoflurane + N_20, or ketamine.

Please cite this article in press as: Muller, L., Destexhe, A. Propagating waves in thalamus, cortex and the thalamocortical system: Experiments and models. J. Physiol. (2012), http://dx.doi.org/10.1016/j.jphysparis.2012.06.005

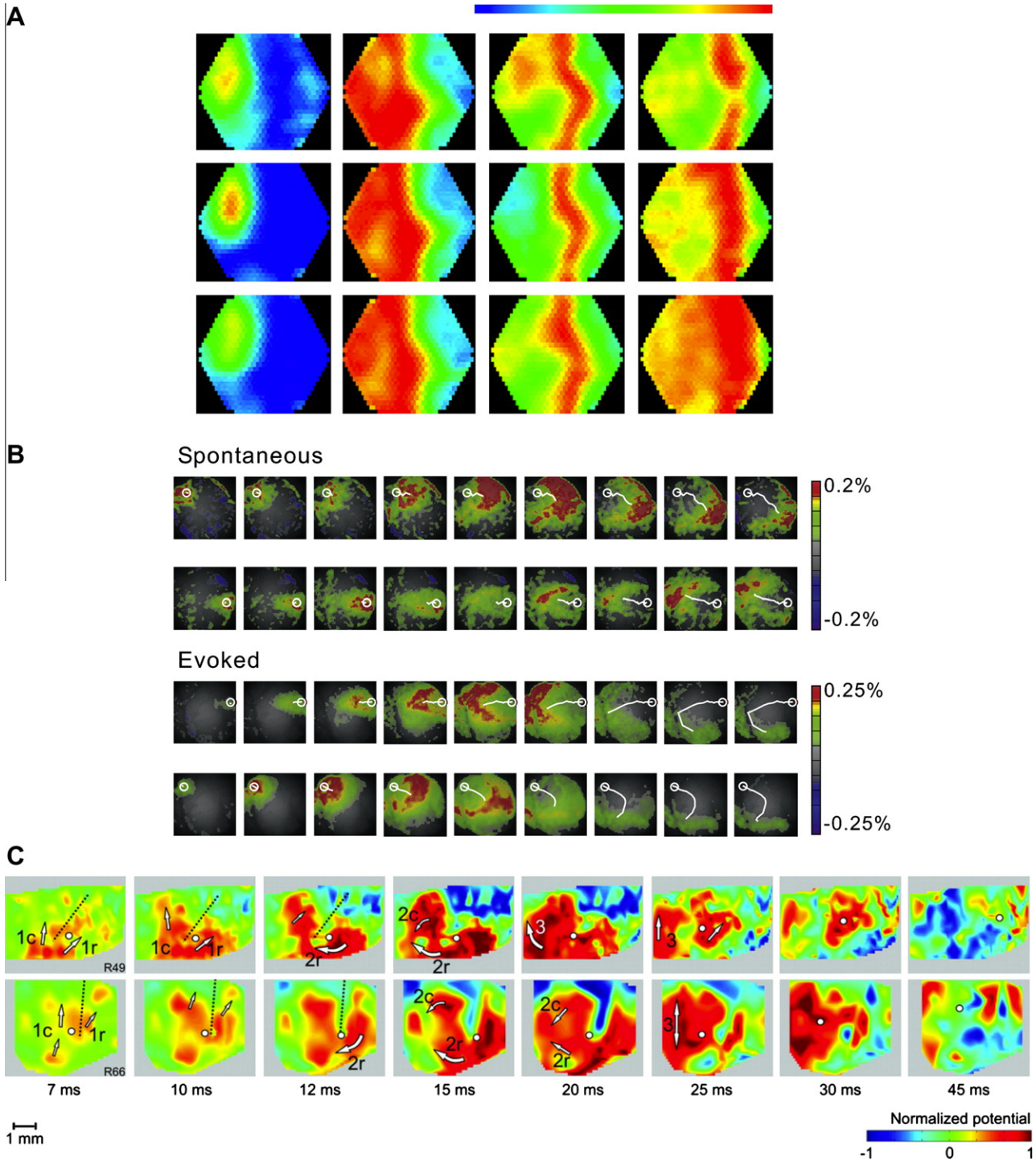

Fig. 3. Propagating waves in cerebral cortex *in vivo* under anesthesia. (A) Three VSDI runs from the same animal demonstrating trial-variability of the spatiotemporal dynamics of propagating waves. The four panels in turn depict initiation, propagation, compression, and reflection of stimulus-evoked waves in the primary visual cortex. The color bar is located above the panels. Adapted from Xu et al. (2007). (B) Spatiotemporal dynamics of propagation compared across spontaneous and evoked conditions with VSD. In this study (Han et al., 2008), spontaneous cortical waves were found to become more similar to the waves evoked by a given stimulus after repeated presentations. Color bars lie to the right of the panels. Open circles indicate the point of generation, and white lines indicate the trajectory of the center of mass during the trial. Adapted from Han et al. (2008). (C) Propagating waves observed with MEA recordings in the auditory cortex of the rat. Interestingly, in this study, onset latencies across the four participating cortical areas were found to be of similar magnitude, in contrast to the classic hierarchical sequential model of cortical processing.

Han et al., 2008; Chavane et al., 2011) or tonotopically (Harel et al., 2000; Versnel et al., 2002; Ojima et al., 2005; Song et al., 2006) organized spatiotemporal activity. Interestingly, it has been recently observed that the onset latency of the propagating waves is similar across auditory cortical areas in the anesthetized rat (Reimer et al., 2010), a result which challenges the notion of feed-forward hierarchy in cortical computations (Fig. 3C).

These waves, however, have been recorded under a myriad of anesthetic conditions, ranging from an almost totally quiescent state, to the UP/DOWN state, and – increasingly – to the desynchronized EEG of the awake state. While it is certain that brain state will have a large effect on the spatiotemporal dynamics of these networks (Destexhe and Paré, 1999; Steriade et al., 2001; Léger et al., 2005), no unified account of the change in propagating

Please cite this article in press as: Muller, L., Destexhe, A. Propagating waves in thalamus, cortex and the thalamocortical system: Experiments and models. J. Physiol. (2012), http://dx.doi.org/10.1016/j.jphysparis.2012.06.005

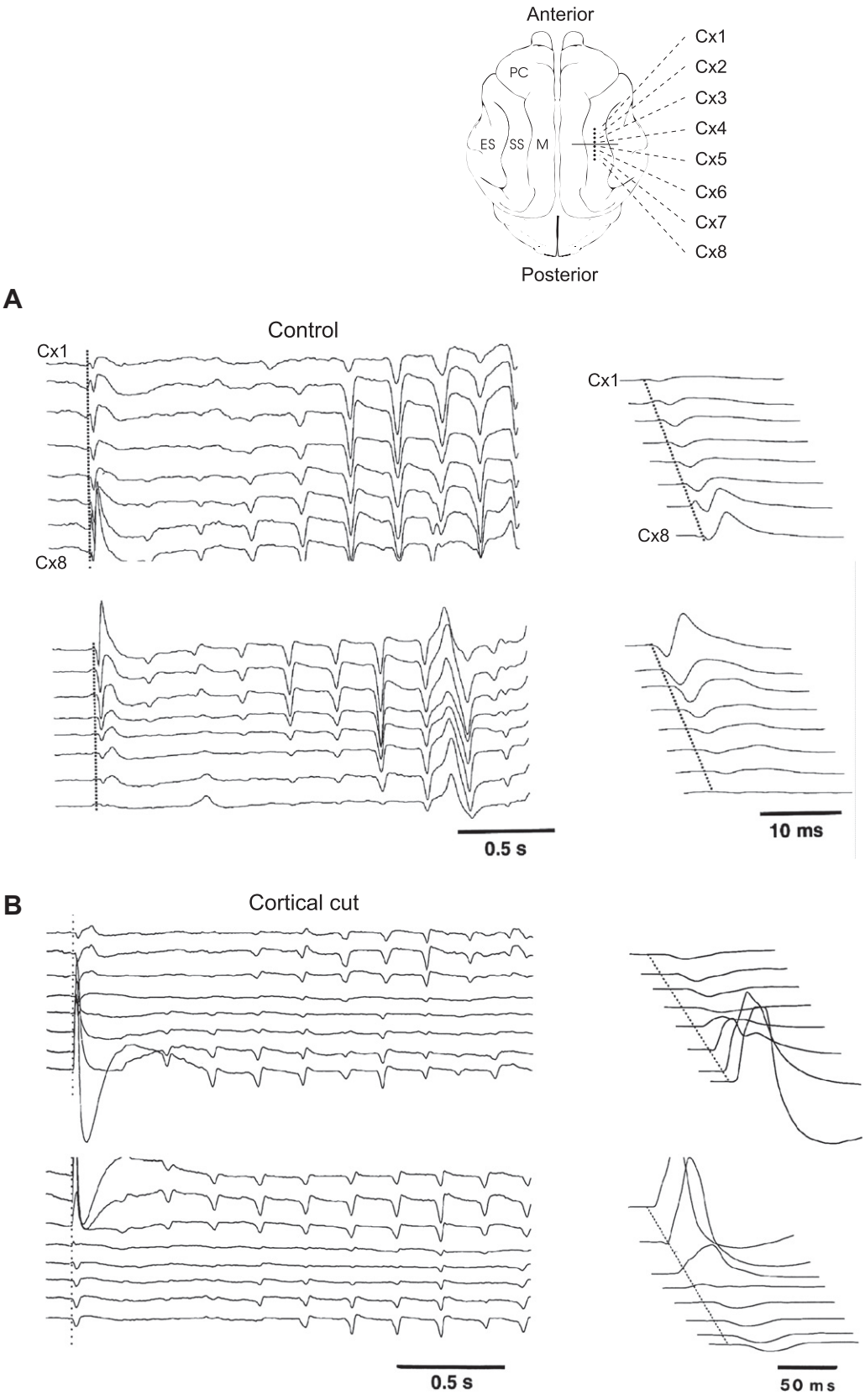

Fig. 4. Propagating waves in cat association cortex *in vivo*. Top: scheme of the recording configuration with eight extracellular electrodes inserted in suprasylvian (SS) cortex in cats anesthetized with barbiturates. (A) Electrical stimulation in the posterior (top) or anterior (bottom) side resulted in propagating spindle waves. (B) Same experiment after a deep cut in cerebral cortex (horizontal bar in top scheme). Although direct corticocortical connections were cut, the propagation still occurred. Modified from Contreras et al. (1997).

Please cite this article in press as: Muller, L., Destexhe, A. Propagating waves in thalamus, cortex and the thalamocortical system: Experiments and models. J. Physiol. (2012), http://dx.doi.org/10.1016/j.jphysparis.2012.06.005

activity as a function of brain state has emerged. Above threshold levels, general anesthetics induce either UP/DOWN or totally quiescent brain states (Franks, 2008), which are characterized by increased adaptation conductances and external input that is either decreased or totally absent. In the neocortical DOWN state, membrane potentials are relatively hyperpolarized and background firing rates are low (Steriade et al., 1993; Destexhe et al., 2003; Destexhe et al., 2003; Léger et al., 2005), reflecting many features of the synapse-poor networks *in vitro*. Because the driving force on synaptic inputs during the DOWN state is high, incoming stimulus-driven spikes to the network will have a large depolarizing effect (Destexhe and Paré, 1999; Léger et al., 2005), causing a localized membrane potential deflection that can spread easily through the quiescent network, unimpeded by ongoing activity.

Finally, propagating waves have also been observed as arising from thalamocortical interactions under barbiturate anesthesia *in vivo*. In the parietal cortex of cats anesthetized with light doses of barbiturates, it was shown that electric stimulation of cerebral cortex can result in triggering spindle oscillations, with propagating properties (Contreras et al., 1997). This propagating wave is illustrated in Fig. 4 and arose from stimulation on either side of the electrode array (Fig. 4A). Interestingly, these propagating oscillatory waves still occur following a deep cut across the whole extent of the cortical gyrus (Fig. 4B). Thus, in contrast to the cortical propagating waves reviewed above, these propagating waves do not critically depend on intracortical connections, and are thought to arise from thalamocortical interactions (see Section 3.1). This emphasizes again the polysynaptic nature of propagating waves involving the thalamus, as we will further see in the modeling section.

2.3. In vivo – awake recordings

Considering the above points on stimulus integration in the neocortical DOWN state, it would be reasonable to expect that the large, low-frequency propagating waves observed during anesthesia would give way to localized bumps of activity in the awake or lightly anesthetized case, where neurons sit a few millivolts below threshold, correlation coefficients of nearby neurons' membrane potentials are suppressed, and background firing rates are somewhat higher than in anesthesia (Destexhe and Paré, 1999; Destexhe et al., 2003; Poulet and Petersen, 2008). In the activated network state, the driving force on synaptic inputs is suppressed, and incoming stimulus-driven spikes will induce smaller EPSPs, causing a smaller local membrane potential deflection when compared to similar stimulation during neocortical DOWNs. Additionally, because of ongoing desynchronized activity in the network, the synchronous depolarization of nearby neurons may be unlikely to spread across the network as a large propagating wave.

The first VSDI results in awake monkeys seem to confirm these expectations (Slovin et al., 2002; Chen et al., 2006; Meirovithz et al., 2010; Ayzenshtat et al., 2010). In these studies, visual stimuli elicit localized peaks of activity whose center of mass remains stationary throughout the response, with the level of activation decaying monotonically with distance. This peak is localized to the point of thalamocortical input, and appears at a latency of 50–100 ms after stimulus onset (Fig. 5A) (Slovin et al., 2002; Chen et al., 2006). While this stationary central peak is a clear feature repeatedly observed in the cortical population response of the awake animal, it is important to note that these first VSDI studies in awake behaving monkeys have presented only trial-averaged data, presumably because of noise constraints, and that the trial-variable spatiotemporal dynamics of propagating waves could be missed under such averaging conditions (Xu et al., 2007). It is important to note additionally that propagating waves of activity have been observed in MEA recordings of the awake cat auditory cortex (Witte et al., 2007), where neurons tend to display properties similar to the low-conductance state of the classic neocortical DOWN across anesthetized and awake conditions (DeWeese and Zador, 2006), and that preliminary evidence for the existence of traveling waves in the spontaneous background activity of the awake state has been presented recently in MEA recordings of the monkey primary visual cortex (Nauhaus et al., 2012). Furthermore, with the advent of new techniques in VSDI denoising that improve the signal-to-noise ratio on the level of single trials (Reynaud et al., 2011), it may presently become possible to detect spontaneous and stimulus-evoked propagating events in VSD recordings from the awake, behaving monkey (Muller et al., in preparation). Finally, at least one study has observed a trend contrary to the expectations for the awake state in the barrel cortex – with depolarization spreading farther and lasting longer in awake mice compared to the anesthetized state (Fig. 5C) (Ferezou et al., 2006). This study, however, also showed stationary spreading depolarization in the somatosensory cortex of the mouse under awake conditions with active perception. From the experimental observations of propagating activity and conductance state across cortical areas, we can see the large extent to which the nature of propagating waves will be shaped by network state, in a manner that depends on stimuli and specific cortical area.

Additionally, the lack of large, low-frequency propagating activity in the awake animal does not preclude the possibility of phase gradients in the high-frequency (20–80 Hz) oscillations classically observed *in vivo* (Gray and Singer, 1989). Indeed, traveling high-frequency oscillations have been observed in MEA recordings of the primary visual cortex (Gabriel and Eckhorn, 2003) and in motor cortex of the awake monkey (Rubino et al., 2006) and human (Takahashi et al., 2011) (Fig. 5B). VSD recordings under similar experimental conditions do not show these high-frequency oscillations (Slovin et al., 2002; Chen et al., 2006; Meirovithz et al., 2010; Ayzenshtat et al., 2010), probably because of the low-pass filtering inherent in the VSD signal (Wu et al., 2001) or stimulus averaging due to noise constraints (Xu et al., 2007). In contrast to the dynamics of the low-frequency propagating waves observed during anesthesia (Sanchez-Vives and McCormick, 2000; Destexhe, 2009), these high-frequency traveling oscillations are likely driven by the interaction between the excitatory and inhibitory populations in the network, as previously proposed (Brunel and Hakim, 1999; Brunel and Wang, 2003). Thus, to reconcile the observations of traveling oscillations in sensory cortices in awake behaving monkeys and the VSDI result of stationary peaks of activation, it must be possible that propagating activity exists throughout the spectrum of network activation, at low frequencies in anesthetized or sleep states and at high frequencies in activated cortical states. These high frequency propagating events may be localized to the central peak of activation, as measured by the VSD signal, or travel farther across the two-dimensional cortical sheet. Interestingly, this hypothesis of large, low-frequency propagating activity in the anesthetized case shifting to smaller, high-frequency propagating activity in the awake case is consistent with observations of increased decay of spatial correlation across the two brain states (Destexhe et al., 1999).

3. Network simulations

3.1. Thalamocortical interactions

Traveling spindle waves were simulated by computational models of networks of interconnected thalamocortical (TC) and thalamic reticular (RE) cells (respectively called LGN and PGN cells in the visual thalamus) in one dimension (see scheme in Fig. 6A), in two independent modeling studies (Destexhe et al., 1996; Golomb

Please cite this article in press as: Muller, L., Destexhe, A. Propagating waves in thalamus, cortex and the thalamocortical system: Experiments and models. J. Physiol. (2012), http://dx.doi.org/10.1016/j.jphysparis.2012.06.005

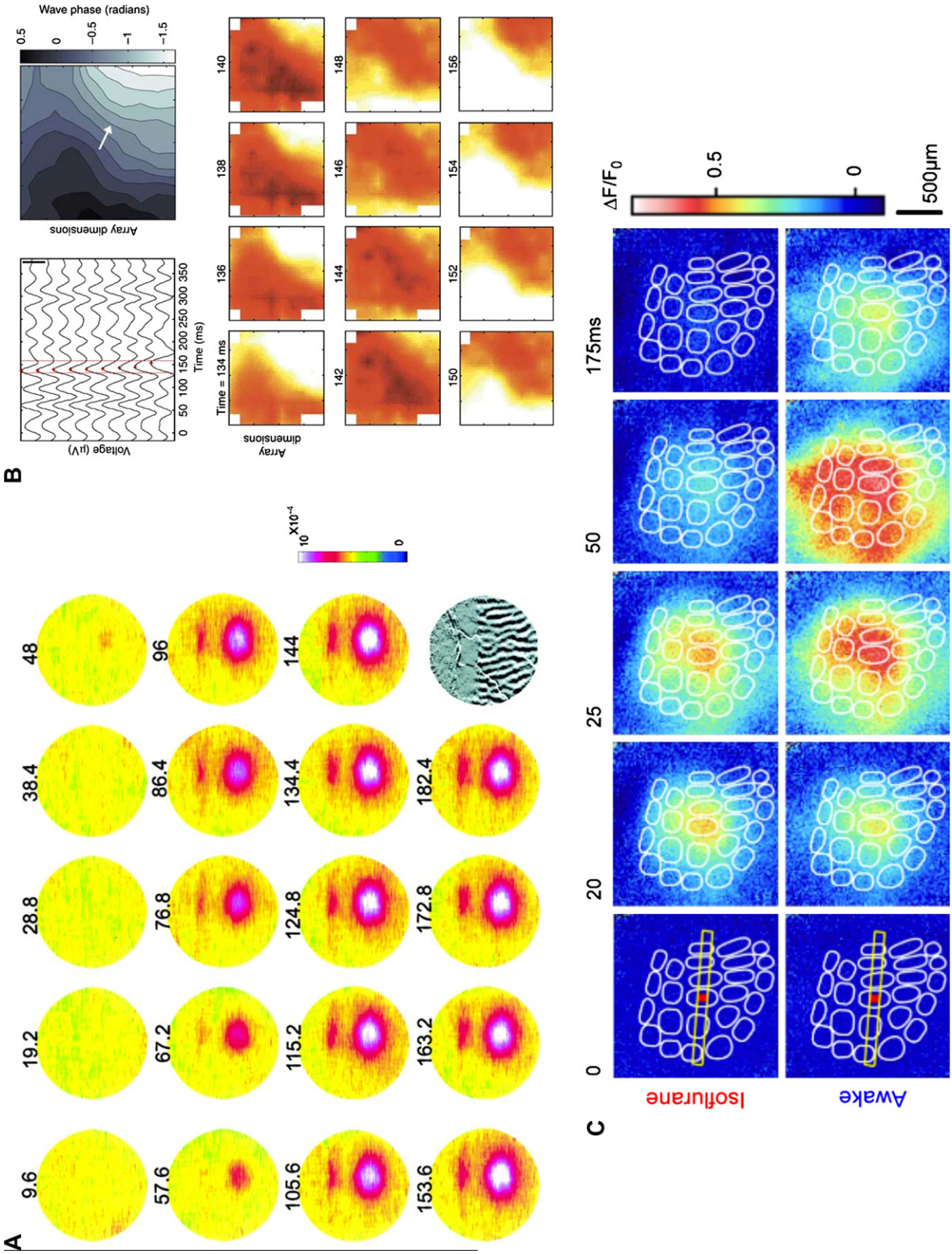

Fig. 5. Propagating waves in the cerebral cortex of awake animals. (A) VSD activation patterns in the primary visual cortex (bottom activity) and secondary visual cortex (top activity) of the macaque in response to a small retinotopic visual stimulus. The V1/V2 border is depicted in the intrinsic ocular-dominance map in the last panel. Time in milliseconds is given above each panel, and the color bar lies to the right. Adapted from Slovin et al. (2002). (B) Beta-band propagating waves observed in MEA recordings of monkey motor cortex (bottom). The top left panel depicts the phase-based method used for measuring propagation speed (not shown) and direction (indicated by white arrow, top right). Isophase contours are depicted in the top right panel, with instantaneous phase across the recording array plotted in grayscale (color bar, top right). Adapted from Rubino et al. (2006) (C) Comparison across isoflurane anesthesia and awake states in VSD recordings of the mouse somatosensory cortex, illustrating the surprising finding that propagating activity spreads farther and lasts longer in awake mice. Color bar is to the right, with spatial scale indicated under the color bar. Adapted from Ferezou et al. (2006).

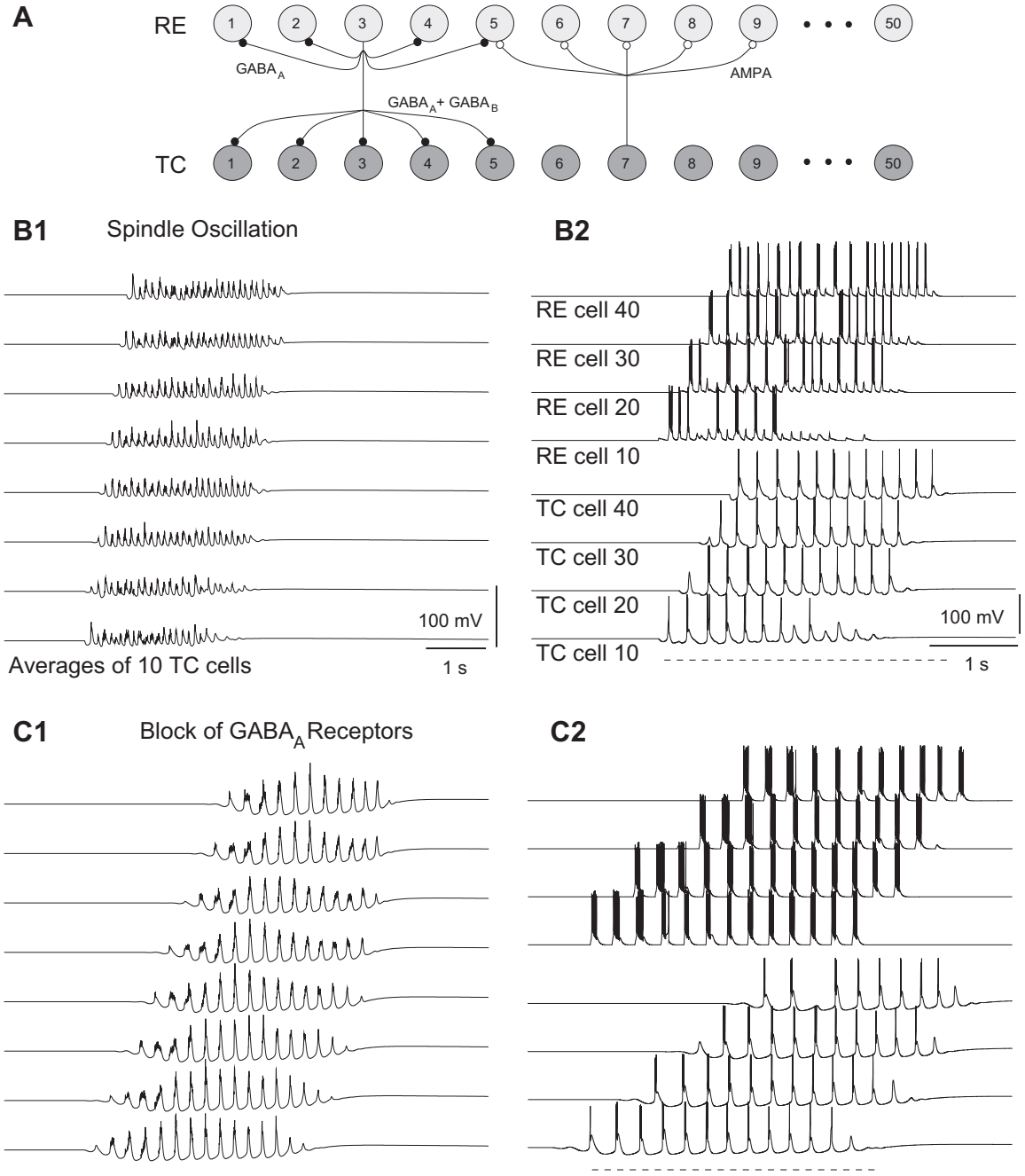

Fig. 6. Network model of propagating waves in thalamic slices. (A) Scheme of the network model, with two types of neurons, thalamocortical (TC) and reticular (RE), interconnected as indicated. (B) Spindle oscillations occurring as an interaction between TC and RE cells. Due to the local connectivity (schematized in A), the oscillation propagated. (C) Slow oscillation following block of $GABA_A$ receptors. The oscillation had a slower frequency and propagated with a lower velocity. Modified from Destexhe et al. (1996).

et al., 1996). These thalamic networks used Hodgkin-Huxley type models of TC and RE neurons, and assumed that there was a topographic connectivity between TC and RE layers, consistent with anatomical data (see details in Destexhe et al. (1996)). Under these conditions, the models generated traveling waves consistent with *in vitro* data (Fig. 6B). Suppression of $GABA_A$ receptors led to slow oscillations around 3 Hz, which propagated at a lower velocity (Fig. 6C), as also observed experimentally.

These models emphasize the fact that the propagating waves observed in thalamic slices (Kim et al., 1995) are the result of polysynaptic interactions involving TC and RE cells. In these models, the spindle oscillation arises from the mutual interaction between TC and RE cells, and the propagating activity involves the simultaneous recruitment of entire populations of neurons, and has therefore a discontinuous character, which gives the appearance of a "lurching wave" (Destexhe et al., 1996; Golomb et al., 1996; Rinzel et al., 1998). This type of wave contrasts with the propagating waves observed in cerebral cortex, which are nearly continuous because they are based on interactions within a relatively homogeneous population.

To investigate propagating waves in the thalamocortical system, a thalamocortical network model was developed by combining the previous model of thalamic slices with a model of deep cortical layers with pyramidal (PY) cells and interneurons (IN)

Please cite this article in press as: Muller, L., Destexhe, A. Propagating waves in thalamus, cortex and the thalamocortical system: Experiments and models. J. Physiol. (2012), http://dx.doi.org/10.1016/j.jphysparis.2012.06.005

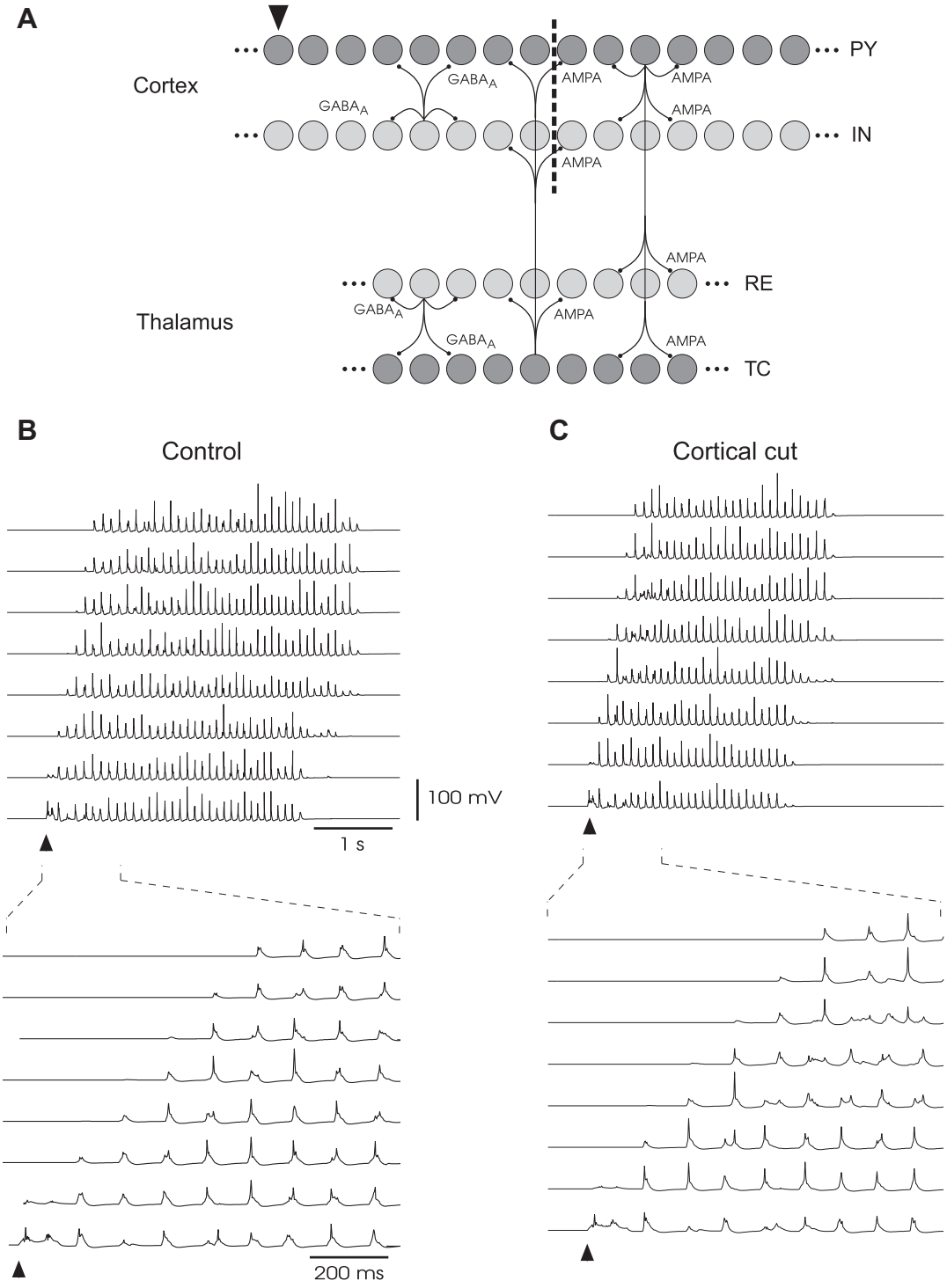

Fig. 7. Network model of propagating waves in the thalamocortical system. (A) Scheme of the network model, with four layer of neurons, cortical pyramidal (PY) cells and interneurons (IN), and thalamic thalamocortical (TC) and reticular (RE) cells. The connectivity between layers was topographic and mediated by glutamate AMPA receptors and $GABA_A$ receptors, as indicated. (B) Control spindle oscillation in the network, and its propagating properties at eight equidistant sites (magnification at the bottom). (C) Same simulation after cutting cortico-cortical connections (dotted line in A). As in experiments, the propagation resisted cutting cortical connections, and involved thalamo-cortical loops. Modified from Destexhe et al. (1998).

(Fig. 7A; see details in Destexhe et al. (1998)). This model could reproduce all experiments on propagating activity, under the assumption that the cortex recruited TC cells primarily through inhibition. This "inhibitory dominant" cortical feedback to the thalamus is consistently observed experimentally, and can explain propagation through thalamocortical loops (Destexhe et al., 1998). In these conditions, the model was capable of reproducing the experiments on evoked traveling waves *in vivo*, as well as their resistance to cutting corticocortical connections (Fig. 7B and C). The same model can also explain the genesis of absence-type of epileptic seizures when the excitability of cortical neurons is too high (Destexhe, 1998). Consistent with this model, propagating activity has indeed been observed in the thalamus of decorticated cats *in vivo* (Contreras et al., 1996).

Please cite this article in press as: Muller, L., Destexhe, A. Propagating waves in thalamus, cortex and the thalamocortical system: Experiments and models. J. Physiol. (2012), http://dx.doi.org/10.1016/j.jphysparis.2012.06.005

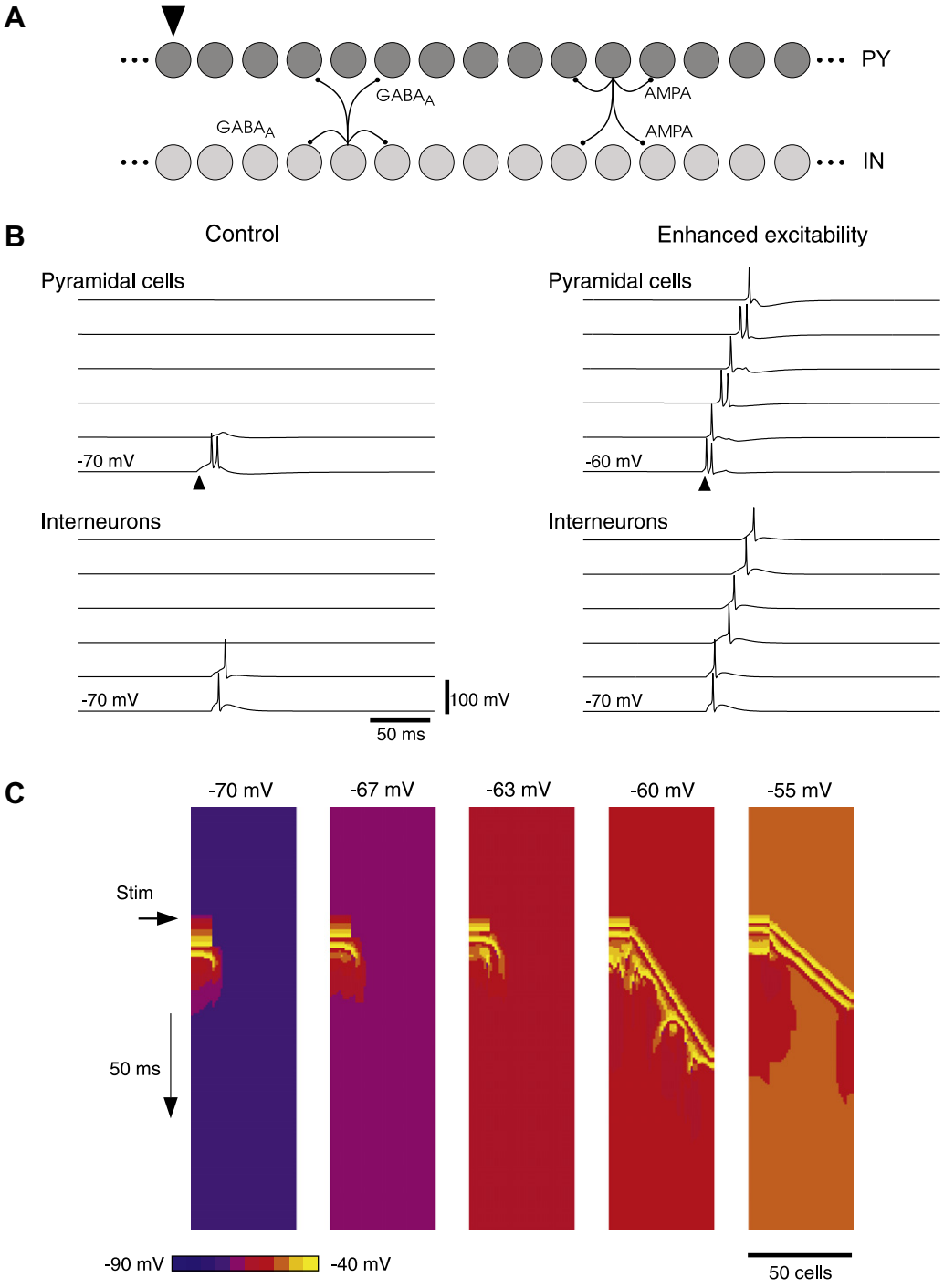

Fig. 8. Network model of propagating waves in cerebral cortex. (A) Scheme of the 1-dimensional network of 50 PY and 50 IN cells, with local axon collateral connections mediated by glutamate AMPA receptors and $GABA_A$ receptors as indicated. (B) Examples of cell activities in the network. In control conditions (left), the resting V_m was of −70 mV and the network did not sustain propagation. With enhanced excitability (right), the more depolarized V_m at −60 mV for PY cells led the network to sustain propagation. (C) Snapshots of activity showing the dependence of propagating activity on the V_m level of PY cells. Modified from Destexhe et al. (1999).

This again emphasizes the polysynaptic aspects of thalamic and thalamocortical propagating waves. In the thalamocortical system, the successive recruitment of larger portions of cortical tissue during the wave depends on several successive synapses:

PY → RE → TC → PY.

The added axonal divergence of each projection is responsible for a marked "lurching" character of these propagating waves, as in the case of the thalamus.

To show the prominent role of cortical excitability, a one-dimensional model was constructed, with PY and IN cells identical to the thalamocortical model above, and with topographical connectivity (Destexhe et al., 1999) (Fig. 8A). This simple cortical model generated monosynaptic propagating waves, in a manner that was critically dependent on the resting membrane potential. For a given connection strength, a propagating wave occurred only at some level (−60 mV in Fig. 8B and C), and the velocity of the wave was also dependent on the resting level of PY cells.

Please cite this article in press as: Muller, L., Destexhe, A. Propagating waves in thalamus, cortex and the thalamocortical system: Experiments and models. J. Physiol. (2012), http://dx.doi.org/10.1016/j.jphysparis.2012.06.005

Table 1
Model parameters.

Simulation parameters		
Parameter class	Parameter	Value (units)
Cell	g_L	16.67 nS
	V_r	−70.0 mV
	V_{reset}	−70.0 mV
	V_{thresh}	−50.0 mV
	T_{refrac}	5.0 ms
	Δ_T	2.5 mV
	τ_w	600.0 ms
	C_m	250.0 pF
	a	1.0 ns
	b (exc)	5.0/155.0 pA
	b (inh)	0.0 nA
Synaptic	E_e	0.0 mV
	E_i	−80.0 mV
	τ_e	2.0/5.0 ms
	τ_i	5.0 ms
Network	L	1.0/2.0/4.0 mm
	v_c	0.2 m/s
	K	400
	K_{exc}	320
	K_{inh}	80
	σ_c	0.2 mm
	ν_{ext}	0–25 Hz
ODE	dt	0.1 ms
	T	2–10 s

In contrast to the "lurching" waves of the thalamus and thalamocortical system seen above, these cortical waves were continuous and were highly dependent on proximity of the mean V_m to spike threshold. Thus, we can infer from these simulations that the genesis of such monosynaptic propagating waves by cortical networks will be sensitive to the excitability of cortical cells, which could be affected by neuromodulatory factors. Propagating wave activity will also be sensitive to any factor that changes the mean V_m of the neurons, such as for example the general "state" of activity of cerebral cortex (Destexhe et al., 2003), as investigated in the next section.

3.2. Corticocortical interactions

To investigate the dependence of propagating waves on "network state", the simulations shown above must be augmented with the ability to display spontaneous activity, to match the high levels of spontaneous activity observed *in vivo* (reviewed in Destexhe et al. (2003)). To address this point, we considered network models displaying more realistic activity states, where input to the system is fundamentally shaped by background activity. For this purpose, we considered a small-scale topographic network ($N = 8000$, with $N_e = 6400$ and $N_i = 1600$). Individual neurons followed the bidimensional adaptive exponential integrate-and-fire (AdEx) model (Brette and Gerstner, 2005), described by the equations:

$$C_m \frac{dV}{dt} = -g_L(V - V_r) + g_L \Delta_T e^{\frac{V - V_T}{\Delta_T}} - w + g_e(t)(E_e - V) + g_i(t)(E_i - V) \quad (1)$$

$$\tau_w \frac{dw}{dt} = a(V - V_r) - w \quad (2)$$

where C_m is the membrane capacitance, g_L is the leak conductance, V_r is the resting membrane potential, Δ_T is the slope factor, V_T is the threshold voltage, g_e and g_i are the time-dependent synaptic conductances, E_e and E_i are the reversal potentials for excitatory and inhibitory synaptic transmission, and w is the adaptation variable. The level of adaptation in this model is specified by parameters a (subthreshold) and b (spike frequency adaptation). At a membrane potential high above threshold, where the exponential nonlinearity dominates, the membrane potential is reset to V_r, and the adaptation variable w is incremented by the spike frequency adaptation parameter b. To ensure against residual synchronization in the network, small Gaussian heterogeneities were incorporated in the C_m, g_L, and V_T parameters. Membrane potentials were randomly initialized from a uniform distribution between V_r and V_T. Additional simulations with randomly initialized w variables in the pyramidal neurons were run to ensure that the results reported were not the result of initial transients. Glutamatergic fast synaptic transmission via AMPA receptors plays a central role in the generation of horizontal propagation *in vitro*, while NMDA receptors have only a modulatory effect.[10] Thus, we chose to consider only fast synaptic conductances, with time constants in the range of 2–5 ms. Conductance changes at individual synapses follow an alpha-function. Parameter values for the AdEx neurons were adapted from Destexhe (2009). A listing of parameter values not explicitly discussed in the text is given in Table 1. All simulations were performed using the PyNN interface (Davison et al., 2008) to the NEST simulation environment (Gewaltig and Diesmann, 2007).

In order to study the spatial aspects of activity propagation, we embedded the network on a one-dimensional ring, with distance-dependent connection probabilities and delays as in previous work (Yger et al., 2011). Connection probabilities between neurons decay as a Gaussian with distance (ℓ_{ij}), following the spatial profile:

$$p_{ij} = e^{-\frac{\ell_{ij}^2}{2\sigma_c^2}} \quad (3)$$

where σ_c is the standard deviation – in this context, the spatial spread – of the Gaussian profile (Mehring et al., 2003). The axonal conduction delay between two neurons (d_{ij}) grows linearly with distance, following the relation:

$$d_{ij} = d_{syn} + \frac{\ell_{ij}}{v} \quad (4)$$

where d_{syn} (0.3 ms) is the minimum synaptic delay, and v is the axonal conduction velocity (0.2 m/s) (Bringuier et al., 1999). Each neuron receives $K_e = 320$ excitatory and $K_i = 80$ inhibitory recurrent synapses from the network drawn from the Gaussian spatial profile, giving 5% connectivity in the case of 8000 neurons. Additionally, we consider that the neuron receives an equivalent number of excitatory synaptic inputs from outside the network (Morrison et al., 2007; Kumar et al., 2008), each firing with a rate ranging from 0 to 25 Hz.

To characterize the results of the network simulations, we considered the mean firing rate, the mean pairwise cross-correlation, and the peak frequency of population oscillations. Mean firing rate is computed as the mean spike count over neurons during the simulation interval; however, because of heterogeneity in the network, some neurons are silent and do not spike during this interval, and these are not included in the mean firing rate estimate (Kumar et al., 2008). Mean pairwise cross-correlation is computed as the normalized zero-lag correlation coefficient averaged across 500 randomly chosen neuron pairs (Aertsen et al., 1989). To characterize the spatiotemporal patterns of subthreshold activity, we recorded the mean membrane potential ($\langle V_m \rangle$) across the network in an array of 10 detectors at intervals of 1 ms.

It has been previously shown that the adaptation present in this neuron model can facilitate the transition from activated, asynchronous irregular (AI) states to UP/DOWNs (Destexhe, 2009); here, we have extended this result to understand the spatial organization of high and low frequency activity across network states. To illustrate the dependence of the spatial structure of activity on the intensity of external Poisson input, we studied these

[10] see Section 2.1 – *in vitro*.

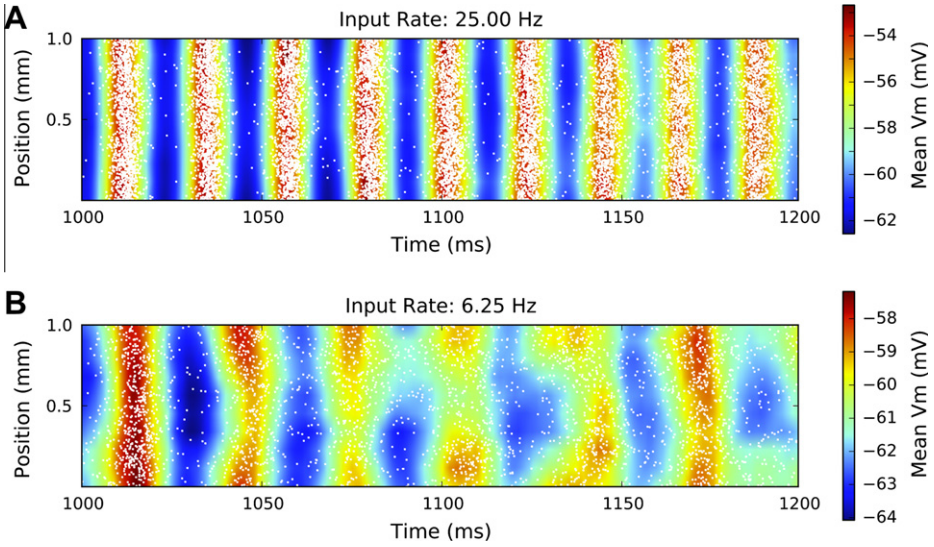

Fig. 9. Short-timescale spatial structure of network population activity driven by external input. In both panels, mean membrane potential in 0.1 mm bins is plotted in false color (color bars at right), and single-unit spikes are plotted in white. (A) Coherent population oscillations. With high external input (individual synapses firing at 25 Hz) and low neuronal adaptation (b – 0.005 nA), the network displays highly synchronized oscillations, with irregular dynamics at the single-neuron level. (B) Traveling oscillations. With lower external input (6.25 Hz), both oscillation frequency and coherence are decreased, revealing clear phase gradients on the level of individual cycles.

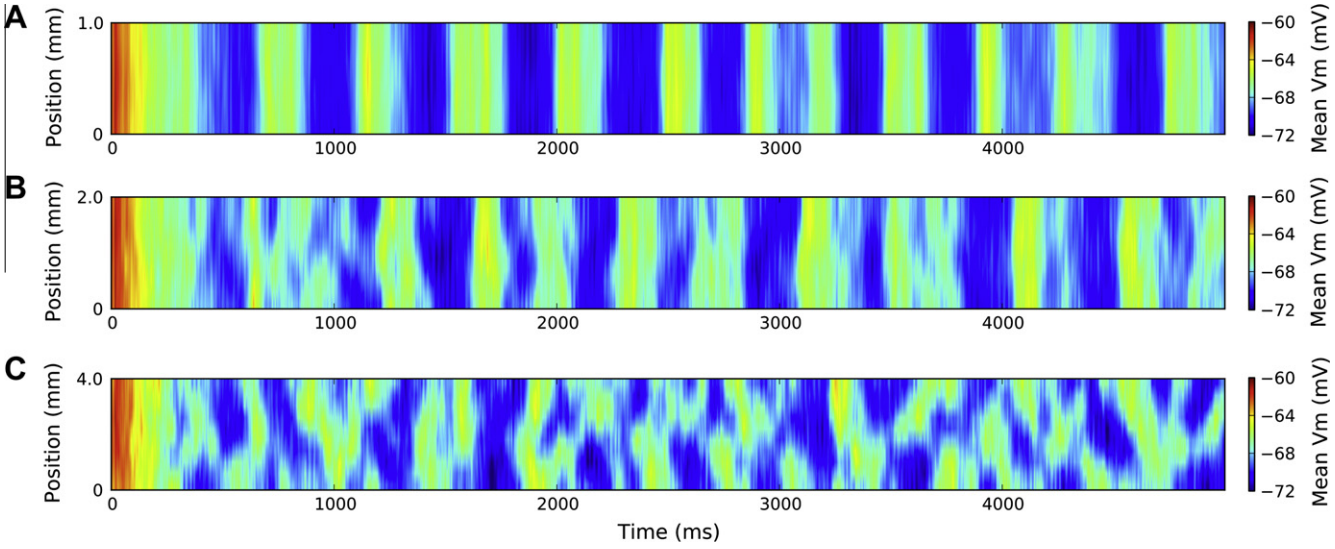

Fig. 10. Scaling of spatial structure in low-frequency oscillations with total network length. The three panels present the results of simulations of coupled one-dimensional ring networks with local connections and conduction delays. Only one layer is depicted here, across three different spatial scales (L = 1, 2, 4 mm). It is important to note the difference in timescales between this and the preceding Fig. (5 s versus 200 ms in Fig. 9). (A) L = 1 mm. In this case, the low-frequency population activity is highly synchronized, with little phase shift across space. (B) L = 2 mm. In this intermediate regime, the scale of the network begins to have a clear effect on the population activity, structuring the oscillations with a gradual phase shift. (C) L = 4 mm. After a second doubling of the network length, the spatial structure of the population activity changes qualitatively, with periods of propagations alternating with periods of incoherent, patchy activity.

small-scale locally connected ring networks in an oscillatory regime (τ_e – 2 ms, τ_i – 5 ms, g_e – 0.8 ns, g – 4) and varied the level of external input across the range of biologically relevant values. Given high external input (ν_{ext} – 25 Hz) and low adaptation (b – 5 pA), the network displays coherent, high frequency oscillations (with a peak at 46 Hz in the power spectrum of multi-unit activity), low single-unit firing rate (11.52 Hz) and low average cross correlation (0.081 $\langle CC \rangle$) at the single-neuron level, consistent with previous theoretical work (Brunel and Hakim, 1999; Brunel and Wang, 2003) (Fig. 9A). With a lower external drive to the system (ν_{ext} – 6.25 Hz), however, network population events have a lower frequency (30 Hz) and become less coherent, producing oscillations that are not fully synchronized, but have a gradual temporal (i.e. phase) shift across space (Fig. 9B), while the firing of individual neurons remains sparse (6.33 Hz) and uncorrelated (0.011 $\langle CC \rangle$).

To probe the spatial structure of self-sustained activity of the type discussed in Destexhe (2009), we studied two-layer ring networks in a self-sustained activity regime (τ_e – 5 ms, τ_i – 5 ms, g_e – 5 ns, g_i – 70 ns) – one layer with weak adaptation (b – 5 pA), the other with stronger adaptation (b – 155 pA) – displaying bistable dynamics resulting from the transient self-sustained activity of one layer being continually reignited by activity in the second layer.[11] It is important to emphasize here that the membrane potential bistability in this model is not solely driven by strong adaptation

[11] Activity was initiated by a short excitatory pulse of external Poisson input to a local section of one layer.

Please cite this article in press as: Muller, L., Destexhe, A. Propagating waves in thalamus, cortex and the thalamocortical system: Experiments and models. J. Physiol. (2012), http://dx.doi.org/10.1016/j.jphysparis.2012.06.005

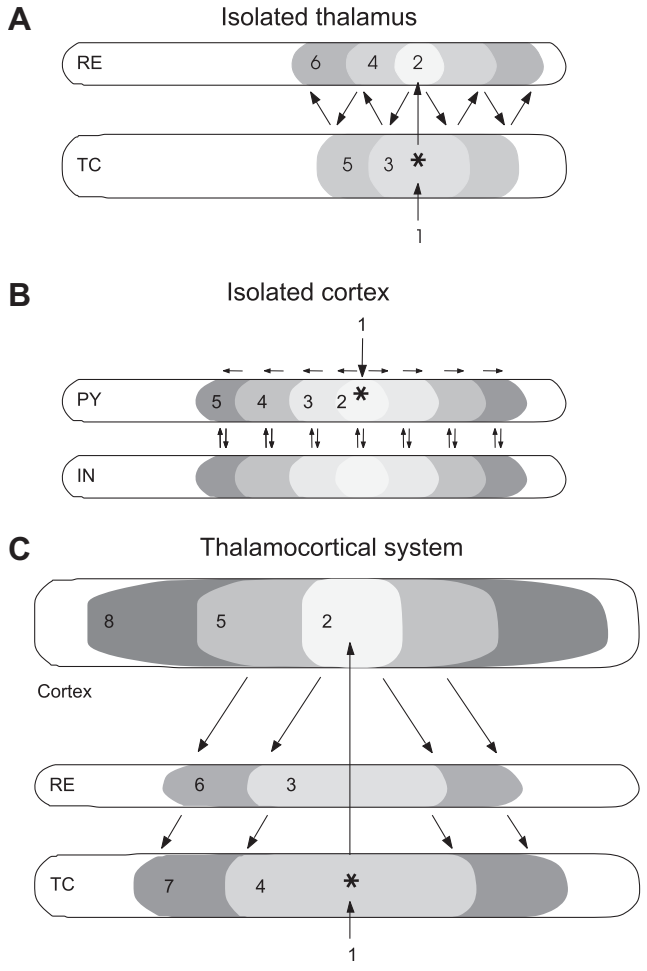

Fig. 11. Different propagation mechanisms in the thalamocortical system. (A) Propagation in the isolated thalamus. The numbers (1), (2), (3),... indicate successive populations of neurons recruited in the propagating wave. In this case, the propagation occurs through successive recruitments between the two layers. (B) Propagation in isolated cortex. In this case, propagation occurs through the local axon collaterals within cortex (horizontal arrows), also recruiting the interneurons (vertical arrows). (C) Propagating waves in the thalamocortical system. The successive recruitments occur through thalamocortical loops. Modified from Destexhe and Sejnowski (2003).

currents, but rather results from an interplay between the self-sustained activity regime at the network level and the adaptation currents at the single neuron level (Destexhe, 2009). To visualize the propagation of the low-frequency oscillations produced in this activity regime, we increased the size of the simulated neural population (N = 112,500, with N_e = 90,000 and N_i = 22,500), with the number of incoming connections per neuron unchanged except for a sparse interlayer excitatory projection (32 synapses per neuron), and systematically changed the length on which the network was wrapped from 1 to 4 mm. Fig. 10 illustrates the change in the spatial structure of population activity with increasing distances in the network. With the original network length (L = 1 mm), the low-frequency population activity is highly synchronized, with very little dependence of the signal on space. After doubling the network length (L = 2 mm), however, the population activity gained a notable shift across space, much greater than that observed in the first case (L = 1 mm). After a second doubling of the network length (L = 4 mm), the population activity again changes qualitatively, with the appearance of incoherent, patchy local activity. This sharp dependence of the structure in population activity on the topology in which the network is embedded during these oscillatory regimes is quite interesting; further considerations, such as the size of the intermediate regime observed here (L = 2 mm), during which coherent yet not fully synchronized population activity is displayed by the network, will be the subject of future study.

Previous studies have begun to address the effect of the topographic nature of cortical networks on their spatiotemporal dynamics (Mehring et al., 2003; Roxin et al., 2005; Kumar et al., 2008; Kilpatrick and Bressloff, 2010; Yger et al., 2011); here, we aim to begin a connection between spiking neural networks with realistic background activity and the experimental results from VSD and MEA recordings taken across brain states. Moreover, whereas topographic models of synfire chain propagation (Mehring et al., 2003; Kumar et al., 2008) or firing rate models with conduction delays (Roxin et al., 2005) focus specifically on propagation of suprathreshold activity, we have focused here on coherent propagation of subthreshold activity, which may be a more robust phenomenon in recurrent networks, specifically in the ongoing activity regime (cf. dissociation between the spatiotemporal patterns in spikes and $\langle V_m \rangle$, Fig. 9B). Additionally, several studies have modeled results from recordings of propagating activity in cortical slices, establishing a detailed connection between propagation and membrane-level conductances, specifically relating their results to the paroxysmal activity state (Golomb and Amitai, 1997; Golomb, 1998; Golomb and Ermentrout, 2002). Here, we aim to study propagation in the context of the activity states observed *in vivo* under normal awake and anesthetized conditions; however, it would be interesting to explore these states in future work. Furthermore, while we have focused predominantly in this work on the activity dynamics of spiking neural networks, it is important to note the substantial literature on propagating waves in neural fields (Ermentrout, 1998; Bressloff, 1999; Goulet and Ermentrout, 2011; Kilpatrick and Ermentrout, 2012) and in networks of coupled oscillators (Kopell and Ermentrout, 1986; Ermentrout and Kleinfeld, 2001), which could provide strong insights into the spatial structure of activity dynamics in spiking neural networks in the future.

Figs. 9 and 10 provide a succinct illustration of possible states for the locally connected networks with conduction delays studied here, as a function of both external input and neuronal adaptation. This model illustrates the transition from low-frequency dominated network states commonly observed during anesthesia and slow-wave (SWS) sleep to high-frequency dominated states observed in waking, activated cortex as an interplay between network-level parameters (e.g. external input rate) and single-unit parameters (level of adaptation). Furthermore, the existence of low-frequency and high-frequency activity need not be mutually exclusive in the model and the two may coexist, consistent with experimental observations of brief high-frequency epochs occurring between the slow-wave complexes of SWS (Destexhe et al., 1999). Finally, it should be noted that while only single points in rather large parameter spaces are presented here as illustrative examples for the purposes of this preliminary study, they serve as a summary of the results of large-scale parameter scans that have been made as part of a forthcoming exhaustive numerical study.

4. Conclusions

4.1. Different "propagating modes" in the thalamocortical system

Fig. 11 summarizes the different types of propagating mechanisms reviewed here. In thalamic slices or in the isolated thalamus, the propagation occurs through mutual recruitment of TC and RE cells, and is therefore polysynaptic. In Fig. 11A, initiation of activity in TC cells (1) recruits a larger population of RE cells (2) due to

Please cite this article in press as: Muller, L., Destexhe, A. Propagating waves in thalamus, cortex and the thalamocortical system: Experiments and models. J. Physiol. (2012), http://dx.doi.org/10.1016/j.jphysparis.2012.06.005

divergence of connectivity, which recruits a larger population of TC cells (3), etc. The propagation occurs through successive recruitments between the two layers, as there are no collateral connections in this system. This gives a discontinuous or "lurching" appearance to the propagating wave. Interestingly, because the polysynaptic recruitment involves GABAergic inhibition and inhibitory-rebound sequences, this type of propagating wave is particularly sensitive to altering of GABA receptors. With $GABA_A$ antagonists, the propagating wave is slower, because the wave then depends on the sole activation of the slower type of ($GABA_B$-mediated) inhibition.

In cerebral cortex (Fig. 11B), the propagation occurs through the abundant excitatory collateral connections, and is therefore essentially monosynaptic. In the example of Fig. 11B, activity initiates in PY cells (1), recruits a larger population of PY cells (2) due to local axon collaterals, which itself recruits an even larger population (3), etc. The interneurons are recruited in parallel by the same collaterals. In this case, because propagation speed depends on excitability and proximity of the V_m to spike threshold, blocking $GABA_A$ inhibition is expected to increase excitability and thus also increase propagation velocity (Wu et al., 2001), which is the opposite effect as in the thalamus.

In the thalamocortical system, polysynaptic propagating waves can also occur through mutual recruitment of thalamus and cortex. This is illustrated in Fig. 11C, where initiation in TC cells (1) recruits a larger population in cortex (2) which recruits larger and larger populations in the thalamus (3 and 4), resulting in a more extended recruited population in in cortex (5), etc. This scheme occurs entirely through thalamocortical loops, and is not critically dependent on corticocortical connections. Note that in the case of the thalamic and thalamocortical propagating activities, the propagation is dependent on an oscillation (generated in the thalamus). The models reviewed here reproduce all these interactions.

4.2. Propagating waves depend on network state

Understanding how the topographic nature of cortical networks influences their dynamics and computational properties is critical for a complete description of stimulus integration and localization in the brain. We have reviewed here the available experimental literature from multichannel recordings to assess the functional significance of propagating waves to the waking, activated state of cortical networks and introduced a computational model whose purpose is to account for the range of spatially structured activity generated from the balance of internal and external drives across brain states. Consistent with this approach, we can account for the transition from long- to short-timescale activity as an interplay between single-neuron and network-level properties.

At this time, several key experimental questions stand ready to be answered, such as the explicit dependence of propagating waves on the brain state of the animal and how these spatiotemporal patterns of activation interact with the cortical maps observed after averaging many trials in electrophysiological or optical recording. Additionally, the spatiotemporal interaction of multiple propagating events across the cortical sheet is an important point to consider in the context of the complexity of naturalistic visual or auditory stimuli.

While we have focused here specifically on the potassium-mediated adaptation conductances affected by anesthesia, it is important to note that many neuromodulatory substances modify conductances at the single-neuron level, and may cause determinable effects at the macroscopic level. The transition from large, low-frequency propagating waves to smaller, high-frequency propagating activity analyzed here is one example of analyzing the spatiotemporal dynamics and stimulus integration of a topographic neural network by considering the network conductance state. Certainly, it is possible to uncover more effects of this type when considering ascending modulatory pathways such as the dopaminergic or noradrenergic systems (Bear et al., 2002), and this is a possibility for future work. Moreover, the influence of top-down inputs mediated by processes such as attention during active perception may be an important consideration when understanding the state-dependent shift in propagating activity (Krupa et al., 2004; Ferezou et al., 2006; Poulet and Petersen, 2008).

Acknowledgments

The authors are grateful to an anonymous reviewer for helpful comments. This work has been supported by the CNRS, the Agence Nationale de la Recherche (ANR HR-Cortex, Complex-V1) and the European Community (FET Grants FACETS FP6-015879, BRAINSCALES FP7-269921). L.M. is a PhD fellow from École des Neurosciences de Paris (ENP).

References

Aertsen, A.M.H.J., Gerstein, G.L., Habib, M.K., Palm, G., 1989. Dynamics of neuronal firing correlation: modulation of "Effective Connectivity". J. Neurophys. 61, 900–917.

Ahmed, B., Hanazawa, A., Undeman, C., Eriksson, D., Valentiniene, S., Roland, P.E., 2008. Cortical dynamics subserving visual apparent motion. Cereb. Cortex 18, 2796–2810.

Ayzenshtat, I., Meirovithz, E., Edelman, H., Werner-Reiss, U., Bienenstock, E., Abeles, M., Slovin, H., 2010. Precise spatiotemporal patterns among visual cortical areas and their relation to visual stimulus processing. J. Neurosci. 30, 11232–11245.

Bear, M.F., Connors, B.W., Paradiso, M.A., 2002. Neuroscience: Exploring the Brain. Lippincott, Williams & Wilkins, Baltimore, MA.

Bressloff, P.C., 1999. Synaptically generated wave propagation in excitable neural media. Phys. Rev. Lett. 82, 2979–2982.

Brette, R., Gerstner, W., 2005. Adaptive exponential integrate- and-fire model as an effective description of neuronal activity. J. Neurophysiol. 94, 3637–3642.

Bringuier, V., Chavane, F., Glaeser, L., Fregnac, Y., 1999. Horizontal propagation of visual activity in the synaptic integration field of area 17 neurons. Science 283, 695–699.

Brunel, N., Hakim, V., 1999. Fast global oscillations in networks of integrate-and-fire neurons with low firing rates. Neural Comput. 11, 1621–1671.

Brunel, N., Wang, X.J., 2003. What determines the frequency of fast network oscillations with irregular neural discharges? I. Synaptic dynamics and excitation–inhibition balance. J. Neurophysiol. 90, 415–430.

Buonomano, D., 2003. Timing of neural responses in cortical organotypic slices. Proc. Natl. Acad. Sci. 100, 4897–4902.

Chagnac-Amitai, Y., Connors, B.W., 1989. Horizontal spread of synchronized activity in neocortex and its control by GABA-mediated inhibition. J. Neurophysiol. 61, 747–758.

Chavane, F., Sharon, D., Jancke, D., Marre, O., Frégnac, Y., Grinvald, A., 2011. Lateral spread of orientation selectivity in V1 is controlled by intracortical cooperativity. Front. Sys. Neurosci., 10.3389/fnsys.2011.00004.

Chen, Y., Geisler, W.S., Seidemann, E., 2006. Optimal decoding of correlated neural population responses in the primate visual cortex. Nat. Neurosci. 9, 1412–1420.

Civillico, E.F., Contreras, D., 2006. Integration of evoked responses in supragranular cortex studied with optical recordings in vivo. J. Neurophysiol. 96, 336–351.

Contreras, D., Destexhe, A., Sejnowski, T.J., Steriade, M., 1996. Control of spatiotemporal coherence of a thalamic oscillation by corticothalamic feedback. Science 274, 771–774.

Contreras, D., Destexhe, A., Sejnowsky, T.J., Steriade, M., 1997. Spatiotemporal patterns of spindle oscillations in cortex and thalamus. J. Neurosci. 17, 1179–1196.

Cruikshank, S.J., Lewis, T.J., Connors, B.W., 2007. Synaptic basis for intense thalamocortical activation of feedforward inhibitory cells in neocortex. Nat. Neurosci. 10, 462–468.

Davison, A.P., Brüderle, D., Eppler, J.M., Kremkow, J., Muller, E., Pecevski, D.A., Perrinet, L., Yger, P., 2008. PyNN: a common interface for neuronal network simulators. Front. Neuroinform., doi:10.3389/neuro.11.011.2008.

Derdikman, D., Hildesheim, R., Ahissar, E., Arieli, A., Grinvald, A., 2003. Imaging spatiotemporal dynamics of surround inhibition in the barrels somatosensory cortex. J. Neurosci. 23, 3100–3105.

Destexhe, A., 1998. Spike-and-wave oscillations based on the properties of $GABA_B$ receptors. J. Neurosci. 18, 9099–9111.

Destexhe, A., 2009. Self-sustained asynchronous irregular states and up/down states in thalamic, cortical and thalamocortical networks of nonlinear integrate-and-fire neurons. J. Comput. Neurosci. 27, 493–506.

Destexhe, A., Paré, D., 1999. Impact of network activity on the integrative properties of neocortical pyramidal neurons in vivo. J. Neurophys. 81, 1531–1547.
Destexhe, A., Sejnowski, T., 2003. Interactions between membrane conductances underlying thalamocortical slow-wave oscillations. Physiol. Rev. 83, 1401–1453.
Destexhe, A., Bal, T., McCormick, D.A., Sejnowski, T.J., 1996. Ionic mechanisms underlying synchronized oscillations and propagating waves in a model of ferret thalamic slices. J. Neurophys. 76, 2049–2070.
Destexhe, A., Contreras, D., Steriade, M., 1998. Mechanisms underlying the synchronizing action of corticothalamic feedback through inhibition of thalamic relay cells. J. Neurophys. 79, 999–1016.
Destexhe, A., Contreras, D., Steriade, M., 1999. Cortically-induced coherence of a thalamic-generated oscillation. Neuroscience 92, 427–443.
Destexhe, A., Contreras, D., Steriade, M., 1999. Spatiotemporal analysis of local field potentials and unit discharges in cat cerebral cortex during natural wake and sleep states. J. Neurosci. 19, 4595–4608.
Destexhe, A., Rudolph, M., Paré, D., 2003. The high-conductance state of neocortical neurons in vivo. Nat. Rev. Neurosci. 4, 739–751.
DeWeese, M.R., Zador, A.M., 2006. Non-Gaussian membrane potential dynamics imply sparse, synchronous activity in auditory cortex. J. Neurosci. 26, 12206–12218.
Ermentrout, E., 1998. The analysis of synaptically generated traveling waves. J. Comput. Neurosci. 5, 191–208.
Ermentrout, G.B., Kleinfeld, D., 2001. Traveling electrical waves in cortex: insights from phase dynamics and speculation on a computational role. Neuron 29, 33–44.
Ferezou, I., Bolea, S., Petersen, C.C.H., 2006. Visualizing the cortical representation of whisker touch: voltage-sensitive dye imaging in freely moving mice. Neuron 50, 617–629.
Franks, N.P., 2008. General anaesthesia: from molecular targets to neuronal pathways of sleep and arousal. Nat. Rev. Neurosci. 9, 370–386.
Fukuda, M., Hata, Y., Ohshima, M., Tsumoto, T., 1998. Role of NMDA receptors in the propagation of excitation in rat visual cortex as studied by optical imaging. Neurosci. Res. 31, 9–21.
Gabriel, A., Eckhorn, R., 2003. A multi-channel correlation method detects traveling γ-waves in monkey visual cortex. J. Neurosci. Methods 131, 171–184.
Gewaltig, M.O., Diesmann, M., 2007. NEST (neural simulation tool). Scholarpedia 2 (4), 1430.
Golomb, D., 1998. Models of neuronal transient synchrony during propagation of activity through neocortical circuitry. J. Neurophysiol. 79, 1–12.
Golomb, D., Amitai, Y., 1997. Propagating neuronal discharges in neocortical slices: computational and experimental study. J. Neurophysiol. 78, 1199–1211.
Golomb, D., Ermentrout, G.B., 2002. Slow excitation supports propagation of slow pulses in networks of excitatory and inhibitory populations. Phys. Rev. E 65, 061911.
Golomb, D., Wang, X.J., Rinzel, J., 1996. Propagation of spindle waves in a thalamic slice model. J. Neurophys. 75, 750–769.
González-Burgos, G., Barrionuevo, G., Lewis, D.A., 2000. Horizontal synaptic connections in monkey prefrontal cortex: an in vitro electrophysiological study. Cereb. Cortex 10, 82–92.
Goulet, J., Ermentrout, G.B., 2011. The mechanisms for compression and reflection of cortical waves. Biol. Cybern. 105, 253–268.
Gray, C.M., Singer, W., 1989. Stimulus-specific neuronal oscillations in orientation columns of cat visual cortex. PNAS 86, 1698–1702.
Grinvald, A., Lieke, E.E., Frostig, R.D., Hildesheim, R., 1994. Cortical point-spread function and long-range lateral interactions revealed by real-time optical imaging of macaque monkey primary visual cortex. J. Neurosci. 14, 2545–2568.
Han, F., Caporale, N., Dan, Y., 2008. Reverberation of recent visual experience in spontaneous cortical waves. Neuron 60, 321–327.
Harel, N., Mori, N., Sawada, S., Mount, R.J., Harrison, R.V., 2000. Three distinct auditory areas of cortex (AI, AII, and AAF) defined by optical imaging of intrinsic signals. NeuroImage 11, 302–312.
Hirsch, J.A., Gilbert, C.D., 1991. Synaptic physiology of horizontal connections in the cat's visual cortex. J. Neurosci. 11, 1800–1809.
Huang, X., Troy, W.C., Yang, Q., Ma, H., Laing, C.R., Schiff, S.J., Wu, J.Y., 2004. Spiral waves in disinhibited mammalian neocortex. J. Neurosci. 24, 9897–9902.
Jancke, D., Chavane, F., Naaman, S., Grinvald, A., 2004. Imaging cortical correlates of illusion in early visual cortex. Nature 428, 423–426.
Kilpatrick, Z.P., Bressloff, P.C., 2010. Spatially structured oscillations in a two-dimensional excitatory neuronal network with synaptic depression. J. Comput. Neurosci. 28, 193–209.
Kilpatrick, Z.P., Ermentrout, B., 2012. Response of traveling waves to transient inputs in neural fields. Phys. Rev. E 85, 021910.
Kim, U., Bal, T., McCormick, D.A., 1995. Spindle waves are propagating synchronized oscillations in the ferret LGNd in vitro. J. Neurophys. 74, 1301–1323.
Kitano, M., Niiyana, K., Kasamatsu, T., Sutter, E.E., Norcia, A.M., 1994. Retinotopic and nonretinotopic field potentials in cat visual cortex. Vis. Neurosci. 11, 953–977.
Kopell, N., Ermentrout, G.B., 1986. Symmetry and phaselocking in chains of weakly coupled oscillators. Commun. Pure Appl. Math. 39, 623–660.
Kral, A., Tillein, J., Hubka, P., Schiemann, D., Heid, S., Hartmann, R., Engel, A.K., 2009. Spatiotemporal patterns of cortical activity with bilateral cochlear implants in congenital deafness. J. Neurosci. 29, 811–827.
Krupa, D.J., Wiest, M.C., Shuler, M.G., Laubach, M., Nicolelis, M.A.L., 2004. Layer-specific somatosensory cortical activation during active tactile discrimination. Science 304, 1989–1992.
Kumar, A., Rotter, S., Aertsen, A., 2008. Conditions for propagating synchronous spiking and asynchronous firing rates in a cortical network model. J. Neurosci. 28, 5268–5280.
Langdon, R.B., Sur, M., 1990. Components of field potentials evoked by white matter stimulation in isolated slices of primary visual cortex: spatial distributions and synaptic order. J. Neurophysiol. 64, 1484–1501.
Léger, J.F., Stern, E.A., Aertsen, A., Heck, D., 2005. Synaptic Integration in rat frontal cortex shaped by network activity. J. Neurophysiol. 93, 281–293.
Maynard, E.M., Nordhausen, C.T., Normann, R.A., 1997. The Utah intracortical electrode array: a recording structure for potential brain–computer interfaces. Electroenceph. Clin. Neurophys. 102, 228–239.
Mehring, C., Hehl, U., Kubo, M., Diesmann, M., Aertsen, A., 2003. Activity dynamics and propagation of synchronous spiking in locally connected random networks. Biol. Cybern. 88, 395–408.
Meirovithz, E., Ayzenshtat1, I., Bonneh, Y.S., Itzhack, R., Werner-Reiss, U., Slovin, H., 2010. Population response to contextual influences in the primary visual cortex. Cereb. Cortex 20, 1295–1304.
Metherate, R., Cruikshank, S.J., 1999. Thalamocortical inputs trigger a propagating envelope of gamma-band activity in auditory cortex in vitro. Exp. Brain Res. 126, 160–174.
Morrison, A., Aertsen, A., Diesmann, M., 2007. Spike-time dependent plasticity in balanced recurrent networks. Neural Comput. 19, 1437–1467.
Muller, L., Reynaud, A., Chavane, F., Destexhe, A., in preparation. Single-trial voltage sensitive dye imaging reveals propagating waves in awake behaving monkey.
Murakoshi, T., Guo, J.Z., Ichinose, T., 1993. Electrophysiological identification of horizontal synaptic connections in rat visual cortex in vitro. Neurosci. Lett. 163, 211–214.
Nauhaus, I., Busse, L., Carandini, M., Ringach, D.L., 2009. Stimulus contrast modulates functional connectivity in visual cortex. Nat. Neurosci. 12, 70–76.
Nauhaus, I., Busse, L., Ringrach, D.L., Carandini, M., 2012. Robustness of traveling waves in ongoing activity of visual cortex. J. Neurosci. 32, 3088–3094.
Ojima, H., Takayanagi, M., Potapov, D., Homma, R., 2005. Isofrequency band-like zones of activation revealed by optical imaging of intrinsic signals in the cat primary auditory cortex. Cereb. Cortex 15, 1497–1509.
Petersen, C.C.H., Grinvald, A., Sakmann, B., 2003. Spatiotemporal dynamics of sensory responses in layer 2/3 of rat barrel cortex measured in vivo by voltage-sensitive dye imaging combined with whole-cell voltage recordings and neuron reconstructions. J. Neurosci. 23, 1298–1309.
Pinto, D.J., Patrick, S.L., Huang, W.C., Connors, B.W., 2005. Initiation, propagation, and termination of epileptiform activity in rodent neocortex in vitro involve distinct mechanisms. J. Neurosci. 25, 8131–8140.
Poulet, J.F.A., Petersen, C.C.H., 2008. Internal brain state regulates membrane potential synchrony in barrel cortex of behaving mice. Nature 454, 881–885.
Reimer, A., Hubka, P., Engel, A.K., Kral, A., 2010. Fast propagating waves within the rodent auditory cortex. Cereb. Cortex. http://dx.doi.org/10.1093/cercor/bhq073.
Reynaud, A., Takerkart, S., Masson, G.S., Chavane, F., 2011. Linear model decomposition for voltage-sensitive dye imaging signals: application in awake behaving monkey. NeuroImage 54, 1196–1210.
Rinzel, J., Terman, D., Wang, X.J., Ermentrout, B., 1998. Propagating activity patterns in large-scale inhibitory neuronal networks. Science 279, 1351–1355.
Roxin, A., Brunel, N., Hansel, D., 2005. he role of delays in shaping spatio-temporal dynamics of neuronal activity in large networks. Phys. Rev. Lett. 94, 238103.
Rubino, D., Robbins, K.A., Hatsopoulos, N.G., 2006. Propagating waves mediate information transfer in the motor cortex. Nat. Neurosci. 9, 1549–1557.
Sanchez-Vives, M.V., McCormick, D.A., 2000. Cellular and network mechanisms of rhythmic recurrent activity in neocortex. Nat. Neurosci. 3, 1027–1034.
Shoham, D., Glaser, D.E., Arieli, A., Kenet, T., Wijnbergen, C., Toledo, Y., Hildesheim, R., Grinvald, A., 1999. Imaging cortical dynamics at high spatial and temporal resolution with novel blue voltage-sensitive dyes. Neuron 24, 791–802.
Slovin, H., Arieli, A., Hildesheim, R., Grinvald, A., 2002. Long-term voltage-sensitive dye imaging reveals cortical dynamics in behaving monkeys. J. Neurophysiol. 88, 3421–3438.
Song, W.J., Kawaguchi, H., Totoki, S., Inoue, Y., Katura, T., Maeda, S., Inagaki, S., Shirasawa, H., Nishimura, M., 2006. Cortical intrinsic circuits can support activity propagation through an isofrequency strip of the guinea pig primary auditory cortex. Cereb. Cortex 16, 718–729.
Steriade, M., Nunez, A., Amzica, F., 1993. A novel slow (<1 Hz) oscillation of neocortical neurons in vivo: depolarizing and hyperpolarizing components. J. Neurosci. 13, 3252–3265.
Steriade, M., Timofeev, I., Grenier, F., 2001. Natural waking and sleep states: a view from inside neocortical neurons. J. Neurophysiol. 85, 1969–1985.
Takahashi, K., Saleh, M., Penn, R.D., Hatsopoulos, N.G., 2011. Propagating waves in human motor cortex. Front. Hum. Neurosci., 5, doi: 10.3389/fnhum.2011.00040.
Tanifuji, M., Sugiyama, T., Murase, K., 1994. Horizontal propagation of excitation in rat visual cortical slices revealed by optical imaging. Science 266, 1057–1059.
Telfeian, A.E., Connors, B.W., 2003. Widely integrative properties of layer 5 pyramidal cells support a role for processing of extralaminar synaptic inputs in rat neocortex. Neurosci. Lett. 343, 121–124.
Versnel, H., Mossop, J.E., Mrsic-Flogel, T.D., Ahmed, B., Moore, D.R., 2002. Optical imaging of intrinsic signals in ferret auditory cortex: responses to narrowband sound stimuli. J. Neurophysiol. 88, 1545–1558.
von Krosigk, M., Bal, T., McCormick, D.A., 1993. Cellular mechanisms of a synchronized oscillation in the thalamus. Science 261, 361–364.
Wester, J.C., Contreras, D., 2012. Columnar interactions determine horizontal propagation of recurrent network activity in neocortex. J. Neurosci. 32, 5454–5471.

Please cite this article in press as: Muller, L., Destexhe, A. Propagating waves in thalamus, cortex and the thalamocortical system: Experiments and models. J. Physiol. (2012), http://dx.doi.org/10.1016/j.jphysparis.2012.06.005

Witte, R.S., Rousche, P.J., Kipke, D.R., 2007. Fast wave propagation in auditory cortex of an awake cat using a chronic microelectrode array. J. Neural Eng. 4, 68–78.
Wu, J.Y., Guan, L., Tsau, Y., 1999. Propagating activation during oscillations and evoked responses in neocortical slices. J. Neurosci. 19, 5005–5015.
Wu, J.Y., Guan, L., Bai, L., Yang, Q., 2001. Spatiotemporal properties of an evoked population activity in rat sensory cortical slices. J. Neurophysiol. 86, 2461–2474.
Xu, W., Huang, X., Takagaki, K., Wu, J.Y., 2007. Compression and reflection of visually evoked cortical waves. Neuron 55, 119–129.
Yger, P., El Boustani, S., Destexhe, A., Frégnac, Y., 2011. Topologically invariant macroscopic statistics in balanced networks of conductance-based integrate-and-fire neurons. J. Comput. Neurosci. 31, 229–245.

Please cite this article in press as: Muller, L., Destexhe, A. Propagating waves in thalamus, cortex and the thalamocortical system: Experiments and models. J. Physiol. (2012), http://dx.doi.org/10.1016/j.jphysparis.2012.06.005